Journal of Engineering Science and Technology
Vol. 10, No. 4 (2015) 461 - 484

ULTIMATE FLEXURAL BEHAVIOUR OF EXTERNALLY PRESTRESSED NEW BEAMS AND DISTRESSED BEAMS

R. SENTHIL[1], R. MANISEKAR[2,]*

[1]Structural Engineering Division, Anna University, Chennai-600025, India
[2]CSIR-Structural Engineering Research Centre, Taramani, Chennai, India-600113
*Corresponding Author: rmanisekar17@yahoo.co.in

Abstract

External prestressing has become a popular technique in retrofitting of distressed concrete structures, mainly bridges. It is being successfully used in segmental construction of new bridges, which is evident in metro constructions and other types of bridges. Tendons used in external prestressing are unbonded tendons and therefore they are analytically treated as internal unbonded tendons. Stress at ultimate in unbonded tendons is the parameter used to evaluate the ultimate flexural capacity of a concrete member prestressed with unbonded tendons. As far as new members are concerned, sufficient research works were carried out on predicting the ultimate flexural behavior and developing equations for finding. Therefore, an in depth review has been done on the subject and the behavioural mechanism regarding evaluating ultimate flexural capacity are discussed. As far as distressed concrete members are concerned, an analytical model has been developed for a cracked RC beams strengthened by external prestressing and validated with experimental data, and the results are presented and discussed. The difference in behavior of externally prestressed new beams and distressed beams strengthened by external pre-stressing are discussed.

Keywords: Analysis, RC beams, Flexure, Strengthening, External prestressing.

1. Introduction

External prestressing is being used widely for new constructions and retrofitting of distressed concrete structures. Moreover, provisions for external tendons (in terms of deviators and anchorages monolithically) are given in internally pre-stressed members to retrofit, if any distress occur in future. As far as retrofitting is

Nomenclatures

C	Resultant compression
C_{shft}	Shift in position of resultant compression
dLt	Change in length of draped tendons due to deflection
d_n	Depth of crack tip
e	Eccentricity
e_{new}	New eccentricity
f_{ak}	Stress in external tendons at decompression
f_{ck}	Cylinder compressive strength
f_{pe}	Effective prestress in external tendons
f_{ps}	Stress in external tendons at ultimate
f_{pu}	Ultimate strength of prestressing steel
f_{pys}	Stress in external tendons at yielding of untensioned steel
f_t	Tensile strength of concrete
f_y	Yield stress of steel
I	Moment of inertia of uncracked section
I_{crack}	Moment of inertia of cracked section
I_{tr}	Moment of inertia of transformed section for RC member
I_{trp}	Moment of inertia of transformed section for externally prestressed member
L_b	Total beam length
L_t	Total tendon length of draped tendons in between anchoring ends (considering straight)
L_{t1}	Total tendon length without deflection (considering single drape at central deviator)
L_{t2}	Total tendon length with deflection (considering single drape at central deviator)
M	Moment of RC member
M_{crack}	Cracking moment of RC member
M_{crp}	Cracking moment of externally prestressed member
M_p	Moment of externally prestressed member
P	Effective prestressing force
$S_{bot,}$ S_{top}	Stress in externally prestressed member at bottom and at top fiber
T	Tensile force in tendon before applying load
t_p	Thickness of end plate
w	Applied load
w_d	Load due to self weight
w_{dk}	Load at decompression
w_{fa}	Load at further distress
y	Deflection of RC member
y_n	Depth of neutral axis
y_p	Deflection of externally prestressed member

Greek Symbols

χ	Curvature at mid span section of RC member
$\varepsilon_{1,}$ ε_2	Principal tensile and compressive strains respectively
ε_{cp}	Strain in concrete at bottom most fiber of RC member
ε_{crack}	Cracking strain in concrete
ε_T	Strain in tendon beyond effective prestressing stage

concerned, external prestressing is one of the major strengthening techniques, being applied for distressed concrete bridges. Apart from bridge field, it is being used for retrofitting of industrial structures also. However, concrete members strengthened by external prestressing behave in a different manner compared to new members particularly with regard to ultimate flexural behaviour. Formation of plastic hinge, stress-increase in external tendons beyond effective prestress, compatibility issues in the analysis and other issues need detailed investigation, which is observed from the literature review, presented in Section 2.0. Analytical solution has been identified for externally prestressed new concrete members. In the present study, an analytical model has been developed for predicting ultimate flexural behavior of distressed concrete beams strengthened by external prestressing, and the results are discussed.

2. Literature Review

2.1. Stress in unbonded tendons of externally prestressed new concrete members

Tendons used in externally prestressed concrete members are analytically being treated as unbonded tendons, and therefore analytical solutions of members prestressed with internal unbonded post-tensioning tendons are applied for externally prestressed members. Various studies were carried out for the past seven decades on predicting stress at ultimate in unbonded tendons, f_{ps}, as it is used for evaluating ultimate flexural behavior of a concrete member prestressed with unbonded tendons. Naaman and Alkhairi [1] performed a state of-the-art review and summarised that stress at ultimate in unbonded tendons f_{ps} is bounded by effective prestress f_{pe} and yield strength of the prestressing tendons f_{py}. Subsequently, Naaman and Alkhairi [2] proposed an equation to predict f_{ps} in unbonded tendons, which is function of the bond reduction coefficient Ω_u and the ratio of the neutral axis at ultimate to the depth of the prestressing steel c/d_{ps}.

Aparicio and Ramos [3] performed an analytical study on 74 externally prestressed concrete bridges using non-linear Finite Element Model, and suggested constant values of Δf_{ps} for incorporation in codes. Ng [4] proposed a modified bond reduction coefficient to predict Δf_{ps}, which accounts for type of loading and second-order effects but independent of span-depth ratio. Diep et al. [5] developed an equation of cable strain on the basis of deformation compatibility, which incorporates the frictional resistance at deviators. Diep et al. [6] predicted the structural behaviour of externally prestressed concrete beams upto the ultimate state using Finite Element algorithm.

Harajli et al. [7] evaluated second order effects for externally prestressed concrete new members and suggested that the second order effect is mainly influenced by the configuration of deviators, profile of the tendons and the magnitude of the inelastic deflection under failure load. Rao and Mathew [8] presented an analytical method for externally prestressed concrete beams, which takes into account the second order effects and friction at deviators. Manisekar and Rao [9] presented a review on behaviour of various types of deviators, which are employed in beams and box girders including reinforcement details, and suggested that tendon slip, frictional resistance, second order effects and ultimate strength are inter related. Aravinthan et al. [10] performed an experimental study, in which they used high eccentricity for external tendons for simple and continuous girders and observed that the continuous girders with linearly transformed tendon profile exhibit the same flexural behaviour irrespective of tendon layout, and the presence of confinement reinforcement enhances the ductility behaviour. Manisekar and Senthil [11] carried out a state of-the-art review and parametric study on stress in internal unbonded tendons and external tendons, and suggested that Δf_{ps} is directly related to formation of plastic hinge, provided equivalent plastic hinge length should be defined accurately.

Harajli [12] proposed an expression for evaluating the equivalent plastic hinge length and proposed methods to predict Δf_{ps} for modifying equations (18-4) and (18-5) of ACI Building Code [13]. Ng and Tan [14] presented a pseudo-section analysis method for analysing a simply supported externally prestressed beams subjected to two-point load, based on the bond reduction coefficient in strain compatibility by taking into account of second order effects.

Kwak and Son [15] developed an analytical method on the basis of relative displacement between the deviators and the concrete matrix, and concluded that the additional primary moment developed by the placement of external tendons causes an increase in ultimate resisting capacity. Au et al. [16] conducted an experimental investigation to study the post-peak behaviour of partially prestressed beams with external tendons using either steel or Aramid FRP (Fibre Reinforced Plastic) tendons as external tendons, and suggested that the reinforcing index ω is a better indicator than *PPR* (Partial Prestressing Ratio).

Pisani [17] developed a numerical model to simulate the behaviour up to collapse of continuous concrete beams prestressed with bonded and external tendons, by adopting a discretization rule to evaluate the rotation of plastic hinges. Based on his model, he suggested that after yielding of the bonded tension reinforcement, curvature is constant along a discrete element of the concrete structure whose length is equal to the development length of that reinforcement. He and Lao [18] proposed a design equation for stress at ultimate in external and internal unbonded tendons using linear relationship between stress increase in unbonded tendons at ultimate and mid span deflection. Du et al. [19] tested concrete beams partially prestressed with CFRP (Carbon Fibre Reinforced Plastic) external tendons and concluded that proper combination of external CFRP tendons with internal reinforcing steel can impart ductility to the beams.

Bennitz et al. [20] tested externally prestressed RC beams with either steel or CFRP tendons by two point monotonic load. They compared their test data with the model of Tan and Ng [21] and Ng [4] and concluded that beams prestressed with CFRP tendons have increased the strength, stiffness and failure load, but have decreased the ductility relative to unstrengthened beams. Researchers, working on external prestressing have adopted the internal unbonded tendon mechanism for analysis and predicted the behaviour. The approaches they adopted are moment-curvature relationship, empirical methods, strain reduction coefficient method, non-linear Finite Element Method and plastic hinge length approach.

The works are Naaman [22], Tan and Ng [21], Harajli et al. [7], Tan et al. [23], Diep et al. [5], Diep et al. [6], Ng [4], and Ghallab and Beeby [24]. However, all the equations displayed unsatisfactory performance in predicting stress in unbonded tendons when they compared with experimental results. Lack of accuracy in evaluating equivalent plastic hinge length is the reason for the unsatisfactory performance of the equations. The equivalent plastic hinge length has been directly or indirectly involved in all the analytical methods mentioned. Therefore, the prediction equations developed using plastic hinge length approach is identified for reviewing, and discussed in the Section 3.0.

2.2. Distressed concrete members strengthened by external prestressing

Harajli [25] tested concrete beam specimens which were earlier cracked and then strengthened by external prestressing, and observed that flexural strength of the strengthened members were increased by 146% and induced deflections were reduced by 75%. Ghallab and Beeby [26] tested twelve prestressed concrete beams strengthened by external tendons using G Parafil rope, out of which three were cracked prior to strengthening. They suggested that if the internal reinforcing steel does not yield at precracked stage, then the strengthened member at ultimate can be analysed as same as uncracked strengthened beams.

Another investigation of the same kind is done by Elrefai et al. [27], in which RC beams were precracked at stages: overloaded (internal steel is yielded) and non overloaded (internal steel is not yielded), then they were strengthened by external prestressing using Carbon-Fibre Reinforced Polymer Tendon. They observed that beams overloaded prior to strengthening did not have discernable effect on the beam fatigue life in comparison with that of non overloaded beam. Antony and Mohankumar [28] investigated the reliability of external prestressing on strengthened beams using only straight tendon profile, which were earlier damaged by corrosion, and observed that stiffness increased in strengthened beams compared to undamaged beam.

Sirimontree and Teerawong [29] tested a full-scale prestressed concrete highway bridge girder with RC deck slab, which was earlier cracked up to the level of inelastic cracked stage for two times and then strengthened by external prestressing, and found that the required external prestressing force to recover structural performance of a damaged girder depends directly on the damage index, which is the ratio of permanent deformation to the crack deformation of the reference undamaged girder. From the review, it can be understood that distressed concrete members strengthened by external prestressing behave differently in ultimate flexural behaviour especially in occurrence of plastic hinge after yielding of reinforcing steel. Compatibility between deformation of concrete and strain in external tendons needs to be introduced, and ultimate flexural behavior of them needs to be predicted. In view of this, an analytical model has been developed to predict the ultimate flexural behaviour of distressed RC beams strengthened by external prestressing and validated using published data, which is presented in Section 4.

3. Plastic Hinge Length Approach

It is well known that ultimate flexural behaviour of concrete members prestressed with unbonded tendons are assessed by the stress at ultimate in unbonded tendons, for which researchers have been using ACI form as follow:

$$f_{ps} = f_{pe} + \Delta f_{ps} \tag{1}$$

Pannell [30] conducted analytical and experimental studies on beams without nonprestressing steel and proposed the Eq. (3) for the stress in the prestressing steel at ultimate, by considering strain compatibility and equilibrium. He made following assumptions: 1) the beam remains in the elastic range upto failure, except in plastic zone; 2) sections plane before bending remain plane during bending; and 3) the strain in the concrete at the steel level is negligible in the elastic zone. He has considered the concrete strain in the plastic zone and assumed the following:

$$\Delta\varepsilon_{cps} = \frac{\Delta l}{L_p} \tag{2}$$

and the proposed equation is:

$$f_{ps} = \frac{q_u}{\rho_p} f'_c \quad \text{MPa} \tag{3}$$

where, $q_u = \dfrac{q_e + \lambda}{1 + 2\lambda}$ and $q_e = \dfrac{A_{ps} f_{pe}}{b d_p f'_c}$, $\lambda = \dfrac{\psi \rho_p \varepsilon_{cu} E_{ps} d_{ps}}{L f'_c}$, $\psi = 10$, $L = L_o = 10c$,

where, $\Delta\varepsilon_{cps}$ is change in strain in the concrete at the level of the prestressing steel, L_p is length of the plastic zone at ultimate, Δ_l is concrete elongation at the level of the prestressing steel that measured within the length of the plastic zone, c is depth of the neutral axis at ultimate, and ε_{cu} is strain in the concrete top fiber at ultimate.

Tam and Pannell [31] have made an experimental study on partially prestressed concrete beams with the span-to-depth ratio ranged from 20 to 45. The main parameters taken for study were, the initial effective prestress in the tendon, amount of prestressing and nonprestressing steel, the span-to-depth ratio and the initial effective prestress. They observed that all beams developed fine cracks similar to those containing bonded reinforcement. Based on their observations, they modified the Eq. (3) and proposed the Eq. (4) for computing f_{ps} for rectangular section, by taking into account the effect of supplementary nonprestressing reinforcement.

$$f_{ps} = \frac{f'_c \left[\dfrac{q_e + \lambda}{1 + \dfrac{\lambda}{\alpha}} - \dfrac{q_s \lambda}{\alpha + \lambda} \right]}{\rho_p} \quad \text{MPa} \tag{4}$$

where, $q_e = \dfrac{A_{ps} f_{pe}}{b d_p f'_c}$, $q_s = \dfrac{A_s f_y}{b d_p f'_c}$, $\lambda = \psi r \varepsilon_u E_s d / L f_{cu}$, $L = L_o = 10.5c$, where $\alpha = 0.85\beta$ (based on cylinder compressive strength) or $\alpha = 0.68\beta_1$ (based on cube compressive strength), β_1 is the stress block reduction factor defined in the ACI Building code.

Gauvreau [32] and Gilliland [33] demonstrated that deformation in the concrete due to shear at the level of the tendon is small in comparison to the deformation due to flexure. Therefore, the contribution of deformation to the increase in tendon stress at each of the high moment zones, could predict a reasonable total stress increase in tendon. Lee et al. [34] described a computational method of the unbonded tendon stress at the flexural failure of a member. They proposed a new equation for f_{ps}, with the consideration of the strain compatibility-moment equilibrium and the plastic hinge length. They derived the equation in such a way that: 1) by obtaining main parameters and their combinations with theoretical study; and 2) determining the coefficients of parameters by regression, using previous test results. They defined the plastic hinge length, as a function of loading type and Span/depth ratio together, in the support of strain compatibility. Finally they proposed the following:

$$f_{ps} = 10{,}000 + 0.8 f_{se} + \frac{1}{15}\frac{\left(A_s' - A_s\right) f_y}{A_{ps}} + 80\sqrt{\frac{d_s}{d_p}\frac{f_c'}{\rho_p}\left[\frac{1}{f} + \frac{1}{L/d_p}\right]} \text{ Psi} \tag{5}$$

in the limit of $f_{se} + 10{,}000 \le f_{ps} \le f_{py}$

Au and Du [35] reinvestigated the equivalent plastic hinge length (L_o) of Pannell's equation and proposed the value of the parameter ϕ as 9.3 after doing data analysis. They further suggested that the value $\phi = 9.3$ could ensure, about 84% of f_{ps} (predicted) values to be on safe side. Finally they adopted the Pannell's approach and proposed the following:

$$f_{ps} = f_{pe} + \frac{0.0279 E_{ps}\left(d_p - c_{pe}\right)}{l_e} \le f_{py} \quad \text{MPa} \tag{6}$$

where $c_{pe} = \dfrac{A_{ps} f_{pe} + A_s f_y}{0.85 \beta_1 f'_c b} \le f_{py}$

Based on the above works, Manisekar and Senthil [11] carried out a parametric study, relating the parameter Δf_{ps} with equivalent plastic hinge length L_o on the assumption: Prestressed concrete members do not experience cracks before the yielding of untensioned reinforcement. Before formation of cracks, tendon stress also does not increase. Further, formation of plastic hinge starts after yielding of the untensioned reinforcement till the concrete crushing at the extreme compressive fiber of the member. The work is given below:

In Fig. 1 Pannell's [30] plastic hinge length ϕc (i.e., $L_o = \phi c$) and the simple parameter of plastic hinge length 1.5 d_p (i.e., L_o = 1.5 d_p) is shown. Seven test results comprise of rectangular sections and T-beam configuartions used are shown in the legend with the variation of loading type (see Fig. 1). Data of single point load is mentioned as f =10, and the data of two point load is mentioned as f=3. Equivalent plastic hinge length, ϕc and 1.5 d_p were calculated based on the data, shown in the legend. It is shown in Fig. 1 that three values are correlated exactly. Further, the ϕc and Δf_{ps} (Data) by the experimental tests (shown in the legend) were compared, as shown in Fig. 2. Here, exactly the same trend of correlation is obtained as in Fig. 1.

It is reported that the plastic hinge length can be directly related to the Δf_{ps}. Then, Chakrabarti's [36] data (two point loads) was used to see the performance of all the prediction equations, using L_o of Lee et al. [35], and L_o of Harajli and Hijazi [37], which are shown in Figs. 3 and 4 respectively. It is seen that no correlation is possible.

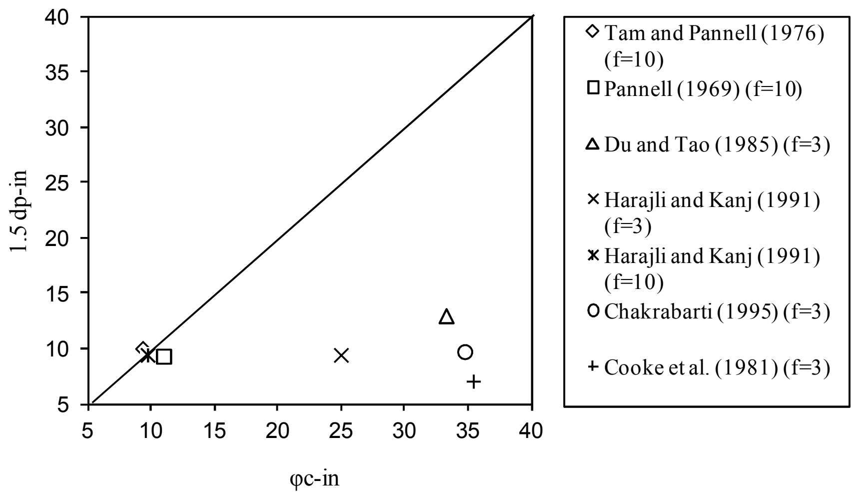

Fig. 1. Comparison of 1.5 d_p with φc of Pannell [30].

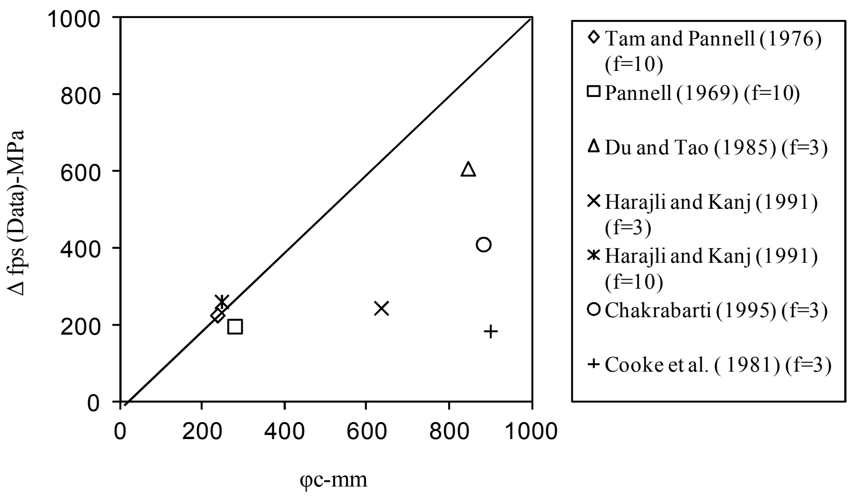

Fig. 2. Comparison of Δf_{ps} (data) with φc of Pannell [30].

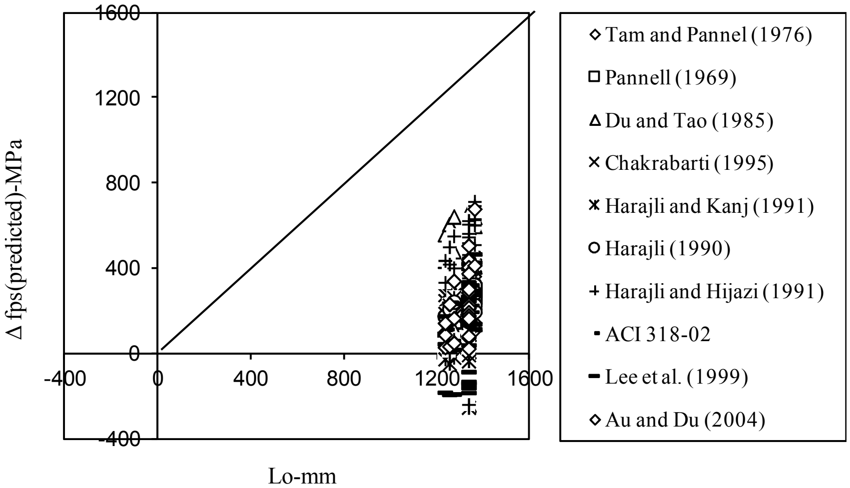

Fig. 3. Comparison of Δf_{ps} (Predicted) with L_0 of Lee et al. [34] (using data of Chakrabarti).

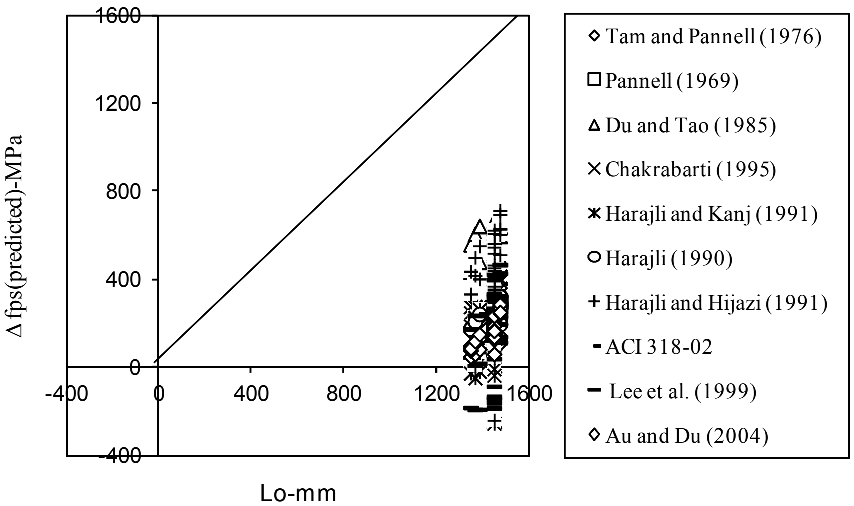

Fig. 4. Comparison of Δf_{ps} (predicted) with L_0 of Harajli and Hijazi [37] (using data of Chakrabarti).

Secondly, the data of Tam and Pannell [31] (subjected to single point load) was taken and made comparisons with L_o of both Lee et al. [34] and Pannell's [30] ϕc, are shown in Figs. 5 and 6 respectively. Here a big improvement is there in correlation when compared to Figs. 3 and 4.

From these comparisons, it can be observed that the inaccuracy in evaluating equivalent plastic hinge length L_o is the reason for the unsatisfactory performance of all the prediction equations, which were used for comparison.

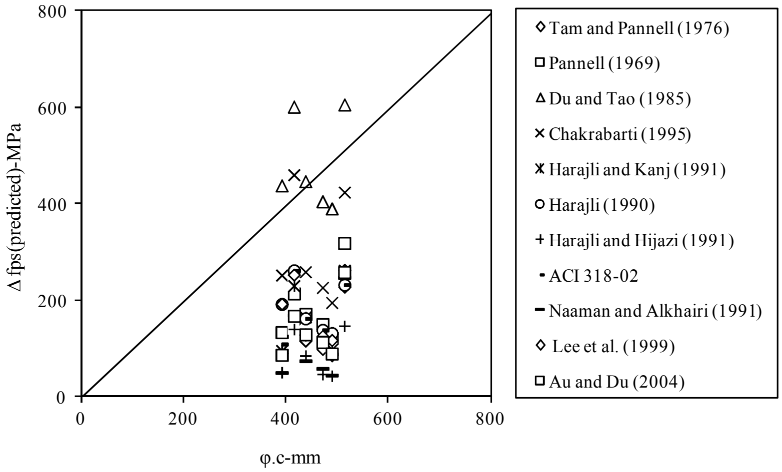

Fig. 5. Comparison of Δf_{ps} (Predicted) with L_0 of Lee et al. [34] (Using data of Tam and Pannell).

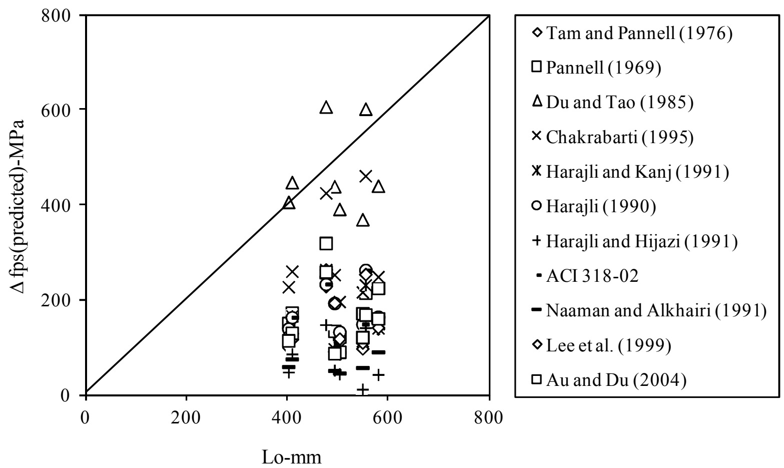

Fig. 6. Comparison of Δf_{ps} (predicted) with L_0 of Pannell [30] (Using data of Tam and Pannell).

Harajli [12] evaluated an equation for equivalent plastic hinge length L_o as $L_o = \left(\frac{20.7}{f} + 10.5\right)c$ and proposed his equation for f_{ps} as follows

$$f_{ps} = \frac{f_{pe} + K_0 E_{ps}\varepsilon_{cu}\left[d_p - \frac{\rho_s d_s f_y}{0.85\beta_1 f_c'}\right]}{1 + \frac{K_0 E_{ps}\varepsilon_{cu}\rho_p d_p}{0.85\beta_1 f_c'}} \quad (7)$$

Therefore, it is observed from the works of Pannell [30], Tam and Pannell [31], Gauvreau [32] and Gilliland [33], Lee et al. [34], Au and Du [35] and Manisekar and Senthil [11] (from Figs. 1 to 6), that stress increase in external tendons for externally prestressed new beams, Δf_{ps}, is directly related to the plastic hinge length, which in the region: from yielding of untensioned reinforcement to concrete crushing in the extreme compressive fiber. However, this conclusion ignored the parameters such as second order effects and slip conditions at deviators of externally prestressed members.

4. Modeling on Strengthened RC Beams by External Prestressing

In the present study, distressed beams consist of rectangular RC beams were considered for modeling. They were cracked and strengthened by external prestressing using single draped tendons. RC beams were cracked to a limit that strain in concrete at extreme fiber varies from 0.0005 to 0.0014, and the strain in reinforcing steel in the limit varies from 0.0015 to 0.00275. That means the reinforcing steel was not yielded. An analytical model was developed and validated with specimens B4D and B5D of experimental data of Harajli [25].

4.1. Compression softening

The deterioration in compression resistance exhibited by the concrete, due to cracking is generally called as compression softening. Since the RC member was cracked earlier, the strength of concrete in compression region would have reduced due to cracking, and therefore, strength reduction of concrete in compression was evaluated. Based on the modified Thorenfeldt base curve (Fig. 7), Vecchio and Collins [38] suggested the compression softening coefficient β as follow:

$$\beta = \frac{1}{1 + K_c} \tag{8}$$

where

$$K_c = 0.27\left(\frac{\varepsilon_1}{\varepsilon_0}\right) - 0.37 \tag{9}$$

$$\varepsilon_0 = \frac{f'_c}{E_c} \tag{10}$$

where ε_0 is strain in concrete cylinder at peak stress f'_c, and E_c is elastic modulus of concrete.

ε_1 is principal tensile strain, computed by referring Modified Compression Field Theory (Vecchio and Collins [39, 40] as follows:

$$\varepsilon_1 = \varepsilon_x + \left[\varepsilon_x + \varepsilon'_c\left(1 - \sqrt{1 - \frac{v}{f'_c}(\tan\theta + \cot\theta)(0.8 + 170\varepsilon_1)}\right)\right]\cot^2\theta \tag{11}$$

where ε_x = longitudinal strain at mid depth of the member (web) in shear region, which was taken as 0.002, permitted by Canadian code [41].

ε'_c = strain in concrete cylinder at peak stress f'_c

shear stress ratio $$v = \frac{V}{b_w jd} \text{ or } v = \frac{V}{\lambda \phi_c f'_c b_v d_v} \quad (12)$$

where $V = \frac{wl}{2} + \frac{W}{2}$

d_v = lever arm, not less than 0.9 d

ϕ_c = material resistance factor

λ = factor to account for density of concrete

for normal density of concrete λ =1.00

for semi-low concrete λ =0.85

for low concrete λ =0.75

θ = inclination of the principal compressive stresses which was calculated using the relation, shear stress ratio (v)-angle of principal compressive stresses (θ) (Colins and Mitchell, [42]), based on longitudinal strain at mid depth, ε_x.

Concrete strength reduction parameter β are calculated as 0.88 and 0.82 for B4D and B5D specimens respectively.

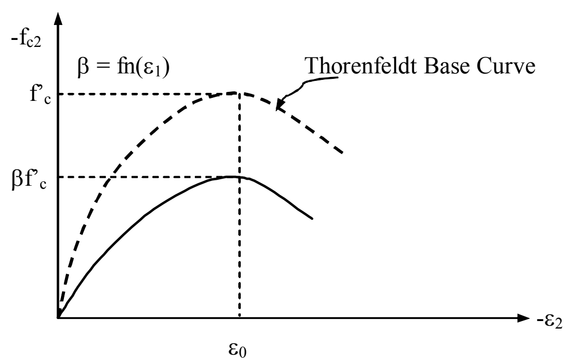

Fig. 7. Modified thorenfeldt base curve-source of compression softening coefficient.

4.2. Analysis of strengthened RC beams by external prestressing (post-strengthening)

Specimen B4D and B5D were having single draped tendons, and deviator was provided at the soffit of the mid span. Normally, external tendons are also treated analytically as unbonded tendons, and therefore analytical status of any member prestressed with external tendons is member dependant and not section dependant [11]. In this investigation, compatibility between deflection at the central deviator location and strain increase in external tendons beyond effective prestress, was applied.

Analysis of externally prestressed cracked RC beams was performed by applying force concept [43]. At the stage of effective prestress, tensile force offered by Tendon, *P*, and the compressive force offered by the resultant compression are in same position. When the moment due to self weight and live load acting upon the member, M_p, the resultant compression shift from the position of tensile force offered by tendons, M_p /P times. Based on the shift in position of resultant compression, eccentricity will go on varying.

Shift in the position of resultant compression = C_{shft}

When there was no any load and no increase in tendon stress, the resultant compressive force and tendon force were same, which was equal to effective prestressing force. Therefore, there was no shift in resultant compression line, which is as follows:

When $C_{shft} = 0$

$$C = T \tag{13}$$

when the position of the resultant compression lies above the tendon line and below the original eccentricity, i.e.,

$$0 \leq C_{shft} < e$$

the distance of the location of resultant compression from the center line of the member (*h/2*), i.e., e_{new} was computed as

$$e_{new} = e - C_{shft} \tag{14}$$

stress in concrete member at top fiber due to external prestressing S_{top} was computed as

$$S_{top} = \frac{P}{A} - \frac{P(e - C_{shft})}{Z_t} \tag{15}$$

Similarly, stress in concrete member at bottom fiber due to external prestressing S_{bot} was computed as

$$S_{bot} = \frac{P}{A} + \frac{P(e - C_{shft})}{Z_b} \tag{16}$$

when the position of the resultant compression is exactly at center line of the member (*h*/2), i.e., when $C_{shft} = e$, then the stress in concrete member at top fiber due to external prestressing S_{top} was computed as

$$S_{top} = \frac{P}{A} \tag{17}$$

Since the C_{shft} is exactly at the centre of the member e_{new} has become zero. Therefore, the second term of Eq. (15) also has become zero. Similarly, stress in concrete member at bottom fiber due to external prestressing S_{bot} was computed as

$$S_{bot} = \frac{P}{A} \tag{18}$$

It was assumed on the basis of experimental data (Harajli [25], which was used for validation) that "the cracks closed due to external prestressing will open only after decompression taking place, and the deflection will start occuring only after cracks opening (i.e., after decompression). Therefore, stress-increase will occur only after decompression takes place since stress-increase strictly bounds by deflection of the member (as deflection compatibility controls the analysis)". Moment of inertia for original section I was used for the analysis of externally prestressed (strengthened) member at stage before decompression, as there is no crack opening before decompression. Whereas Moment of Inertia for transformed section I_{trp} was used for the analysis of externally prestressed (strengthened) member at stage after decompression, as there is crack opening after decompression. The following analysis was done based on the above assumption:

when the position of resultant compression is above the center line of the member, i.e., $0 < e < C_{shft}$, the decompression used to happen, and therefore tension creates at bottom fiber of the concrete member and compression creates at top fiber of the concrete member.

Therefore,

$$S_{top} = \frac{P}{A} + \frac{P(C_{shft} - e)y_t}{I_{trp}} \tag{19}$$

Similarly, stress in concrete member at bottom fiber due to external prestressing S_{bot} was computed as

$$S_{bot} = \frac{P}{A} - \frac{P(C_{shft} - e)y_b}{I_{trp}} \tag{20}$$

4.2.1. Deflection of strengthened cracked RC beams

When the applied load is such that the member does not come to the decompression stage, i.e., $0 < w \leq w_{dc}$

$$y_p = -\frac{Pe_{new}L^2}{12E_{cp}I} \tag{21}$$

When the applied load is such that the member reached the decompression stage, but not reached the further distressing stage, i.e., $w_{fd} > w \geq w_{dc}$

(Reason for using the term 'further distress' is explained in section 4.2.3)

Deflection of the externally prestressed cracked RC beams y_p was computed as

$$y_p = -\frac{Pe_{new}L^2}{12E_{cp}\phi_1 I_{trp}} + kL^2\left[\frac{M_{dc}}{E_{cp}I} + \frac{M - M_{dc}}{0.85E_{cp}\phi_1 I_{trp}}\right] + \frac{5}{384}\frac{w_d L^4}{E_{cp}\phi_1 I_{trp}} \tag{22}$$

When the applied load is such that the member is reached decompression stage and also the further distressing stage, i.e., $w \geq w_{fd} > w_{dc}$ then the deflection of the externally prestressed cracked RC beams y_p was computed as

$$y_p = -\frac{Pe_{new}L^2}{12E_{cp}\phi_2 I_{trp}} + kL^2\left[\frac{M_{dc}}{E_{cp}I} + \frac{M - M_{dc}}{0.85E_{cp}\phi_2 I_{trp}}\right] + \frac{5}{384}\frac{w_d L^4}{E_{cp}\phi_2 I_{trp}} \tag{23}$$

where

$$I_{trp} = \left(\frac{M_{dc}}{M_p}\right)^3 I + \left[1 - \left(\frac{M_{dc}}{M_p}\right)^3\right] I_{crack}$$

$$I_{crack} = \frac{b.d_{np}{}^3}{3} + m.A_{st}(d - d_{np})^2$$

Φ_1 = reduction factor for moment of inertia of transformed section for the stage from load at decompression to load at further distress.

Φ_2 = reduction factor for moment of inertia of transformed section for the stage from load at further distress to the load at ultimate.

4.2.2. Stress in external tendons

For specimen B4D and B5D, deflection compatibility was applied for computing stress in external tendons at ultimate as follow:

Total length of tendon in between anchorages (considering straight), as shown in Fig. 8(a)

$$L_t = L_b + 2t_p \tag{24}$$

Total length of tendon without deflection (considering single drape at central deviator), as shown in Fig. 8(a)

$$L_{t1} = 2\sqrt{e^2 + \left(\frac{L_t}{2}\right)^2} \tag{25}$$

when $w < w_{dc}$

$$L_{t2} = L_{t1} \tag{26}$$

Total length of tendon with deflection (considering single drape at central deviator), shown in Fig. 8(b) is calculated as follows:

when $w \geq w_{dc}$

$$L_{t2} = 2\sqrt{(e + y_p)^2 + \left(\frac{L_t}{2}\right)^2} \tag{27}$$

Then the change in length of tendon is computed as:

$$dL_t = L_{t2} - L_{t1} \tag{28}$$

Strain in tendons is computed as:

$$\varepsilon_t = \frac{dL_t}{L_{t1}} \tag{29}$$

Stress-increase in external tendons is computed as:

$$\Delta f_{ps} = \varepsilon_t E_{ps} \tag{30}$$

where ε_t is computed using equations from Eqs. (24) to (29)

Therefore, stress at ultimate in external tendons is computed, which is in ACI form (ACI 318-2008), as follow:

$$f_{ps} = f_{pe} + \Delta f_{ps} \tag{31}$$

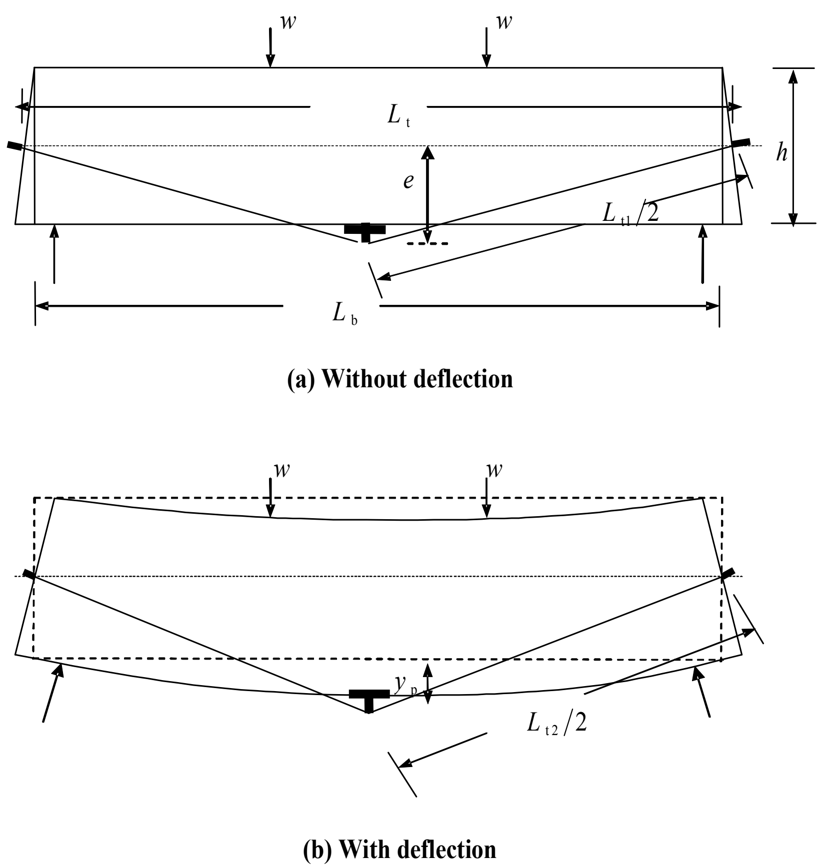

Fig. 8. Strengthened beam with draped tendons.

Stress-increase in external tendons for externally prestressed cracked RC beams was observed at the stage from decompression stage to yielding of untensioned reinforcement. Therefore, stress in external tendons at ultimate state was computed using the Eq. (31).

4.2.3. Validation with experimental data

Specimens B4D and B5D of data of Harajli [25] were used for validation. Material properties for specimens B4D and B5D are given in Table 1. Cross sectional details for specimens B4D and B5D are shown in Figs. 9 and 10 respectively. For details of longitudinal view, Fig. 8 can be referred.

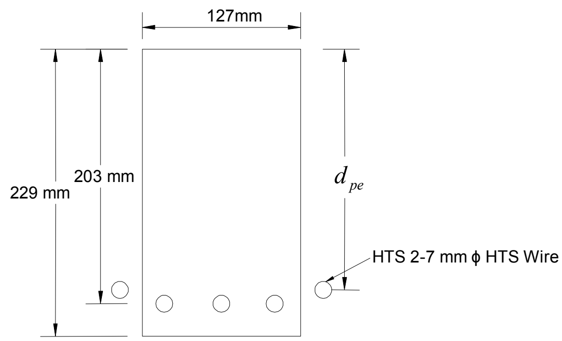

Fig. 9. Cross-sectional details of the specimen B4D.

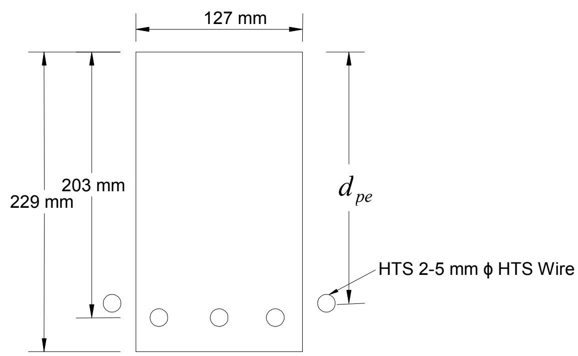

Fig. 10. Cross-sectional details of the specimen B5D.

Table 1. Material properties for specimens B4D and B5D.

Specimens	Reinforcing steel			External prestressing steel				
	No. of Bars	Area of steel mm^2	Yield stress of steel MPa	No. of wires	Area of prestressing steel A_{ps} mm^2	Effective prestress f_{pe} MPa	Ultimate strength of prestressing steel f_{pu} MPa	Compressive strength of concrete f'_c MPa
B4D	2-10 mm	157	310.3	2-5 mm	39.27	879.11	1606.54	30.34
B5D	3-12 mm	339	551.6	2-7 mm	76.97	841.20	1427.27	32.40

The tendon profile is a draped one and the depth of external tendons at mid span, d_{pe}, is 273 mm. The thickness of end plate is 19 mm, which is a tapered one. In both the specimens, untensioned steel was not allowed to yield, before strengthening. Based on the experimental data, external prestressing was done when the beams were subjected to 30% of the calculated ultimated load. Further the specimens were subjected to monotonic load, after strengthening by external prestressing. Shift of neutral axis towards bottom due to external prestressing, which is named here as depth of crack tip from extreme compressive fiber, d_n, was computed by regression method. The d_n is 70 mm and 105 mm for specimens B4D and B5D respectively.

Comparison of results with experimental data for specimen B4D (ext. pre) and B5D (ext. pre) are furnished in Tables 2 and 3 respectively. It was observed that decompression in externally prestressed cracked beams occurred at 24% and 24.9% of ultimate load for B4D and B5D respectively, and yielding of untensioned reinforcement occurred at ultimate load, for both specimens. It was found generally for both specimens (B4D and B5D) that the stress-increase in external tendons, Δf_{ps} , is at stage from decompression to yielding of untensioned reinforcement. Secondly, It was also observed that strengthened member exhibited three stages of behaviour viz., i) from the effective prestressing stage to the load at decompression, w_{dc} ; ii) from the load at decompression w_{dc} to load at further distress w_{fd}; and iii) from the load at further distress w_{fd} to load at ultimate w_u. Amount in deflection was divided into two stages after decompression, and therefore the stage after decompression was named 'further distress' as it showed large deflection.

Table 2. Comparison of results with experimental data of strengthened cracked RC beams by external prestressing for specimen B4D (ext.pre).

Applied load w kN	Stress-increase in external tendons Δf_{ps} (model) MPa	Stress-increase in external tendons Δf_{ps} (exp) MPa	Ratio $\frac{\Delta f_{ps}(\text{exp})}{\Delta f_{ps}(\text{model})}$	Deflection y_p (model) mm	Deflection y_p (exp) mm	Ratio $\frac{y_p(\text{exp})}{y_p(\text{model})}$
3.5	0	0	0	9.67	9.91	1.02
7.6	33.33	39.30	1.18	12.66	12.19	0.96
12	101.71	101.36	0.99	18.16	15.49	0.85
16.55	203.14	155.14	0.76	26.00	18.54	0.71
19.5	274.08	196.51	0.72	31.3	22.10	0.71
20.5	298.49	260.63	0.87	33.08	27.43	0.83
21.75	434.66	338.55	0.78	42.74	33.53	0.78
22.7	466.54	404.05	0.87	44.93	41.40	0.92
23.15	481.70	442 .66	0.92	45.96	53.30	1.16
Mean			0.887			0.884
Standard deviation			0.149			0.149
Coefficient of variation			16.77%			16.89%

It was sensed from the iterations and results that there was necessity to control the deflection in terms of moment of inertia for transformed section, I_{trp}, so as to predict the stress in external tendons, since deflection compatibility ruled the analysis. Accordingly, reduction factors for I_{trp} for second stage and third stage were introduced as ϕ_1 and ϕ_2 respectively. For specimen B4D, the reduction factors ϕ_1 and ϕ_2 for I_{trp}, were 0.82 and 0.72 respectively. For specimen B5D, the reduction factors ϕ_1 and ϕ_2 were 1.00 and 0.76 respectively.

Moment-deflection curve and Moment- Δf_{ps} curve, are shown in Figs. 11 and 12 respectively for specimen B4D. Figures 13 and 14 show the Moment-deflection curve and Moment- Δf_{ps} curve for specimen B5D respectively. They show good agreement with experiment results.

Table 3. Comparison of results with experimental data of strengthened cracked RC beams by external prestressing for specimen B5D (ext. pre).

Applied load w kN	Stress-increase in external tendons Δf_{ps} *(model)* MPa	Stress-increase in external tendons Δf_{ps} *(exp)* MPa	Ratio $\frac{\Delta f_{ps}(\exp)}{\Delta f_{ps}(model)}$	Deflection y_p *(model)* mm	Deflection y_p (exp) Mm	Ratio $\frac{y_p(\exp)}{y_p(model)}$
9.99	0	0	0	7.01	7.11	1.01
15.01	41.26	22.75	0.55	10.51	8.89	0.85
20.60	56.84	61.37	1.08	11.78	11.94	1.01
23.79	103.62	88.26	0.85	15.52	13.46	0.87
29.99	149.46	137.21	0.92	19.11	16.51	0.86
33.00	172.19	160.65	0.93	20.86	18.54	0.89
36.39	198.20	186.86	0.94	22.84	20.32	0.89
40.01	225.94	208.23	0.92	24.93	22.61	0.91
42.50	245.32	226.85	0.92	26.38	24.13	0.91
45.00	264.80	248.22	0.94	27.82	25.91	0.93
47.50	284.38	266.84	0.94	29.26	28.45	0.97
48.19	289.88	286.14	0.99	29.66	30.48	1.03
Mean			0.908			0.928
Standard deviation			0.1305			0.064
Coefficient of variation			14.37%			6.88%

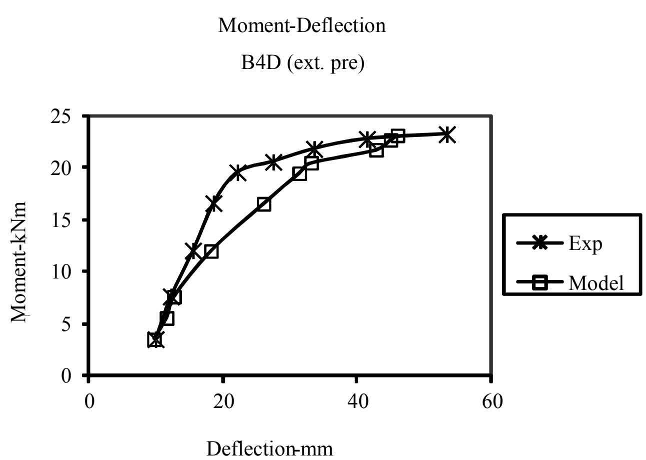

Fig. 11. Moment-deflection curve for specimen B4D (ext. pre).

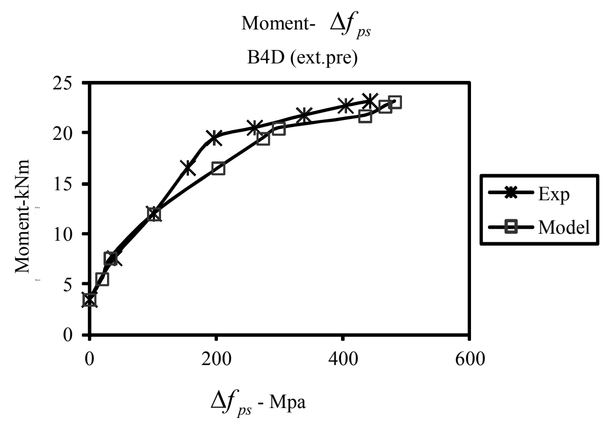

Fig. 12. Moment- Δf_{ps} curve for specimen B4D (ext. pre).

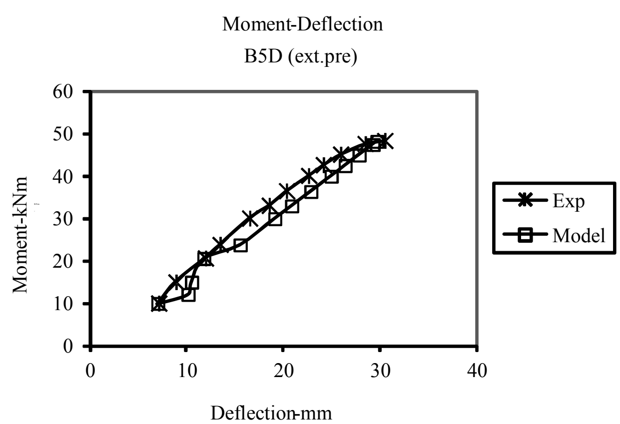

Fig. 13. Moment-deflection curve for specimen B5D (ext. pre).

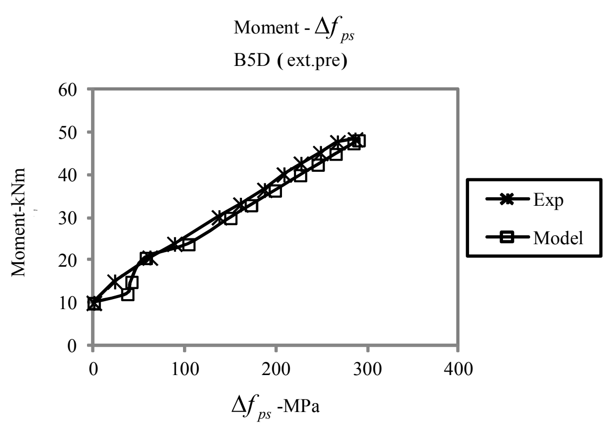

Fig. 14. Moment- Δf_{ps} curve for specimen B5D (ext.pre)

5. Conclusions

In summary the following conclusions have been drawn:

- Stress increase in external tendons for externally prestressed new beams, Δf_{ps}, is directly related to equivalent plastic hinge length, which is in the stage: from yielding of untensioned reinforcement to concrete crushing in the extreme compressive fiber.
- Stress-increase in external tendons for strengthened RC beams, Δf_{ps}, is at stage from decompression to yielding of untensioned reinforcement, provided the extent of the damage is limited that untensioned steel is not yielded.
- Externally prestressed new beams could be analysed using internal unbonded tendon mechanism, except parameters associated with deviators. Accordingly, Δf_{ps} can be calculated using ACI form (Eq. 1), in which Δf_{ps}, is directly related to equivalent plastic hinge length.
- Distressed beams strengthened using external prestressing cannot be analysed using internal unbonded tendon mechanism. Therefore, Δf_{ps} can be calculated using Eq. (30), in which stress-increase in tendons, Δf_{ps}, is at stage from decompression to yielding of untensioned reinforcement.
- Distressed beams strengthened using external prestressing exposed three stages of behaviour after attaining decompression.
- While externally prestressed new beams display plastic hinge before failure, distressed beams strengthened using external prestressing display very little plastic hinge and raise doubts for ductility.

Acknowledgements

Authors are grateful to Dr. Ing. N. Rajagopalan Chief Technical Advisor (Bridges) of L & T Ramboll Consulting Engineers Ltd, Chennai, India, and Dr. D. S. Ramachandramurthy, Principal, St. Peter's College of Engineering and Technology, Chennai-54, India, for their valuable suggestions on this research. Authors are thankful to Dr. Nagesh R Iyer, Director, CSIR-SERC, Chennai, for permitting the paper for publication.

References

1. Naaman, A.E.; and Alkhairi, F.M. (1991). Stress at ultimate in unbonded post-tensioning tendons: Part 1 - Evaluation of the state-of-the-art. *ACI Structural Journal*, 88(5), 641-651.
2. Naaman, A.E.; and Alkhairi, F.M. (1991). Stress at ultimate in unbonded post-tensioning tendons: Part 2 - Proposed methodology. *ACI Structural Journal,* 88(5), 683-692.
3. Aparicio, A.C.; and Ramos, G. (1996). Flexural strength of externally prestressed concrete bridges. *ACI Structural Journal*, 93(5), 512-523.
4. Ng, C.K. (2003). Tendon stress and flexural strength of externally prestressed beams. *ACI Structural Journal*, 100(5), 644-653.
5. Diep, B.K.; Tanabe, T.; and Umehara, H. (2001). Study on behaviour of externally prestressed concrete beams using the deformation compatibility of

cable. *Journal of Materials, Concrete Structures, Pavements, JSCE*, 51(676), 159-168.

6. Diep, B.K.; Umehara, H.; and Tanabe, T. (2002). Numerical analysis of externally prestressed concrete beams considering friction at deviators. *Journal of Materials, Concrete Structures*, *Pavements*, *JSCE*, 57(718), 107-119.
7. Harajli, M.H.; Khairallah. N.; and Nassif, H. (1999). Externally prestressed members: evaluation of second order effects. *Journal of Structural Engineering, ASCE*, 125(10), 1151-1161.
8. Rao, P.S.; and Mathew, G. (1996). Behaviour of externally prestressed concrete beams with multiple deviators. *ACI Structural Journal,* 93(4) 387-396.
9. Manisekar, R.; and Rao, M.V.B. (2003). Behaviour of deviators in external prestressing. *Indian Concrete Journal***,** 77(9), 1332-1338.
10. Aravinthan, T.; Witchukreangkrai, E.; and Mutsuyoshi, H. (2005). Flexural behaviour of two-span continuous prestressed concrete girders with highly eccentric external tendons. *ACI Structural Journal*, 102(3), 402-411.
11. Manisekar, R.; and Senthil, R. (2006). Stress at ultimate in unbonded post-tensioning tendons for simply supported beams- A state of-the-art-review. *Advances in Structural Engineering*, 9(3), 321-335.
12. Harajli, M.H. (2006). On the stress in unbonded tendons at ultimate: Critical assessment and proposed changes. *ACI Structural Journal*, 103(6), 803-812.
13. ACI Committee 318 (2008). *Building code requirements for reinforced concrete*. American Concrete Institute, Detroit, Michigan.
14. Ng, C.K.; and Tan, K.H. (2006). Flexural behaviour of externally prestressed beams. part I: analytical model. *Engineering Structures,* 28(4), 609-621.
15. Kwak, H.G.; and Son, J.K. (2010). Inelastic behavior of PSC beams with unbonded external tendons. *Magazine of Concrete Research*, 62(5), 313-326.
16. Au, F.T.K.; Su, R.K.L.; Tso, K.; and Chan, K.H.E. (2008). Behaviour of partially prestressed beams with external tendons. *Magazine of Concrete Research*, 60(6) 455-467.
17. Pisani, M.A. (2009). Numerical analysis of continuous beams prestressed with external tendons. *Journal of Bridge Engineering*, *ASCE*, 14(2), 93-101.
18. He, Z.; and Liu, Z. (2010). Stresses in external and internal unbonded tendons: unified methodology and design equations. *Journal of Structural Engineering*, *ASCE*, 136(9), 1055-1065.
19. Du, J.S.; Dong, Y.; Ng, P.L.; and Au, F.T.K. (2011). Response of concrete beams partially prestressed with external unbonded carbon fiber-reinforced polymer tendons. *Advanced Materials Research Volumes*, Trans Tech Publications, Switzerland, 150-151.
20. Bennitz, A.; Jacob, W.S.; Jonny, N.; Björn, T.; Per, G.; and Dorthe, L.R. (2012). Reinforced concrete T-beams externally prestressed with unbonded carbon fiber-reinforced polymer tendons. *ACI Structural Journal*, 109(4), 521-530.
21. Tan, K.H.; and Ng, C.K. (1997). Effects of deviators and tendon configuration on behaviour of externally prestressed beams. *ACI Structural Journal*, 94(1), 13-22.

22. Naaman, A.E. (1990). A new methodology for the analysis of beams prestressed with external or unbonded tendons. *External prestressing in bridges*, SP-120, American Concrete Institute, Detroit, 339-354.
23. Tan, K.H.; Al Farook, M.A.; and Ng, C.K. (2001). Behaviour of simple-span reinforced concrete beams locally strengthened with external tendons. *ACI Structural Journal*, 98(2), 174-183.
24. Ghallab, A.; and Beeby, A.W. (2004). Calculating stress of external prestressing tendons. *Proceedings of the Institution of Civil Engineers, Structures & Buildings*, 157(SB 4), 263-278.
25. Harajli, M.H. (1993). Strengthening of concrete beams by external prestressing. *PCI Journal,* 38(6), 76–88.
26. Ghallab, A.; and Beeby, A.W. (2002). Ultimate strength of externally strengthened prestressed beams. *Proceedings of the Institution of Civil Engineers, Structures and Buildings*, 152(4) 395-406.
27. Elrefai, A.; West, J.; and Soudki, K. (2008). Effect of overloading on fatigue performance of reinforced concrete-beams strengthened with externally post-tensioned carbon-fibre-reinforced polymer tendons. *Canadian Journal of Civil Engineering*, 35(11), 1294-1307.
28. Antony, J.C.; and Mohankumar, G. (2008). Strengthening by external prestressing. *Concrete International*, 30(10), 61-66.
29. Sirimontree, S.; and Teerawong, J. (2010). Flexural behaviour of damaged full-scale highway bridge girder strengthened by external post tension. *American Journal of Engineering and Applied Sciences*, 3(4), 650-662.
30. Pannell, F.N. (1969). The ultimate moment of resistance of unbonded prestressed concrete beams. *Magazine of Concrete Research*, 21(66), 43-54.
31. Tam, A.; and Pannell, F.N. (1976). The ultimate moment of resistance of unbonded partially prestressed reinforced concrete beams. *Magazine of Concrete Research*, 28(97), 203-208.
32. Gaureau, D.P. (1993). *Ultimate limit state of concrete girders prestressed with unbonded tendons*. Bericht nr.198, Institutfur Baustatik und Konstruktion, ETH, Zurich, Switzerland..
33. Gilliland, J.A. (1994). *Truss model for predicting tendon stress at ultimate in unbonded partially prestressed concrete beams*. M.Sc. Thesis. Queen’s University, Kingston, Ontario, Canada.
34. Lee, L.H.; Moon, J.H.; and Lim, J.H. (1999). Proposed methodology for computing of unbonded tendon stress at flexural failure. *ACI Structural Journal,* 96(6), 1040-1048.
35. Au, F.T.K.; and Du, J.S. (2004). Prediction of ultimate stress in unbonded prestressed tendons. *Magazine of Concrete Research*, 56(1), 1-11.
36. Chakrabarti, P.R.; Whang, T.P.; Brown, W.; Arsad, K.M.; and Amezeua, E. (1994). Unbonded post-tensioning tendons and partially prestressed beams. *ACI Structural Journal*, 91(5), 616-625.
37. Harajli, M.H.; and Hijazi, S.A. (1991). Evaluation of the ultimate steel stress in partially prestressed concrete members. *PCI Journal*, 36 (1), 62-82.

38. Vecchio, F.J.; and Collins, M.P. (1993). Compression response of cracked reinforced concrete. *ASCE Journal of Structural Engineering*, 119(12), 3590-3610.
39. Vecchio, F.J.; and Collins, M.P. (1986). The modified compression field theory for reinforced concrete elements subjected to shear. *ACI Journal*, 83(2), 219-231.
40. Vecchio, F.J.; and Collins, M.P. (1988). Predicting the response of reinforced concrete subjected to shear using modified compression field theory. *ACI Structural Journal*, 85(3), 258-268.
41. CSA (Canadian Standard Association) (1994). A23.3-94 *Design of concrete structures*. Rexdale, Ontario, Canada.
42. Collins, M.P.; and Mitchell, D. (1986). A rational approach to shear design-The 1984 canadian code provisions. *ACI Journal*, 83(6), 925-933.
43. Rajagopalan, N. (2005). *Prestressed concrete* (2^{nd} Ed.). New Delhi: Narosa Publishing House.